Mechanistic Studies on Rhodium-Catalyzed Carbonylation Reactions: Spectroscopic Detection and Reactivity of a Key Intermediate, $[MeRh(CO)_2I_3]^-$

Anthony Haynes,[1a] Brian E. Mann,[1a] George E. Morris,[1b] and Peter M. Maitlis*,[1a]

Contribution from the Department of Chemistry, University of Sheffield, Sheffield S3 7HF, England, and Research and Development Department, BP Chemicals, Salt End, Hull HU12 8DS, England

Received November 30, 1992

Abstract: The catalytic intermediate $[MeRh(CO)_2I_3]^-$ (**B**) (present to the extent of ca. 1% of **A** at steady state) has been spectroscopically detected in the reaction of $[Rh(CO)_2I_2]^-$ (**A**) with neat MeI giving $[Rh(CO)(COMe)I_3]^-$ (**C**) (Scheme II). FTIR and low-temperature ^{13}C NMR spectroscopic measurements using both ^{13}CO- and $^{13}CH_3$-labeled complexes, and the analogy to $[MeIr(CO)_2I_3]^-$ all favor a fac,cis stereochemistry for **B**. Measurement of the steady-state ratio [**B**]/[**A**] and the pseudo-first-order rate constant for conversion of **A** into **C** has allowed k_2 to be estimated (5–35 °C). Activation parameters for migratory insertion (**B** → **C**) are $\Delta H^{\ddagger} = 63 \pm 2$ kJ mol^{-1} and $\Delta S^{\ddagger} = -59 \pm 9$ J mol^{-1} K^{-1}. The ratio k_2/k_{-1} is estimated to be ca. 9 in CH_2Cl_2 at 35 °C from measurements of the solution behavior of **C**. Activation parameters for the overall reaction of **A** with neat MeI are $\Delta H^{\ddagger} = 50 \pm 1$ kJ mol^{-1} and $\Delta S^{\ddagger} = -165 \pm 4$ J mol^{-1} K^{-1}. Kinetic measurements (15–35 °C) for isotopic label scrambling in $[Rh(^{12}CO)(^{13}COMe)I_3]^-$ give activation parameters for deinsertion (**C** → **B**) of $\Delta H^{\ddagger} = 100 \pm 1$ kJ mol^{-1} and $\Delta S^{\ddagger} = -5 \pm 4$ J mol^{-1} K^{-1}. Complete rate data for the reaction shown in Scheme II at 35 °C are $k_1 = 6.8 \times 10^{-5}$ M^{-1} s^{-1} (MeI), $k_{-1} = 1.5 \times 10^{-2}$ s^{-1} (CH_2Cl_2), $k_2 = 1.33 \times 10^{-1}$ s^{-1} (MeI), and $k_{-2} = 4.20 \times 10^{-5}$ s^{-1} (MeI). Derived equilibrium constants ($K_1 = 4.5 \times 10^{-3}$ M^{-1}, $K_2 = 3.2 \times 10^3$ (35 °C)) show that **B** is unstable with respect to both migratory insertion and reductive elimination of MeI. Rhodium methyl intermediates analogous to **B**, such as $[MeRh(CO)_2Cl_2I]^-$, have been detected in the reaction between $[Rh(CO)_2Cl_2]^-$ and MeI to give $[Rh(CO)_2I_2]^-$ and MeCl, indicating that halide exchange occurs via an oxidative addition/reductive elimination sequence.

Introduction

The low-pressure rhodium- and iodide-catalyzed carbonylation of methanol is one of the most important industrial applications of homogeneous transition metal catalysis.[2] A substantial proportion of the 5 million tons of acetic acid made annually uses this process, and the industrial carbonylation of methyl acetate to acetic anhydride also now employs similar technology.[3] After announcement of the process by the Monsanto company in 1968,[4] studies by Forster[5] and others[6-8] led to formulation of the catalytic cycle shown in Scheme I. High-pressure IR spectroscopy showed that the most prevalent complex in catalytic solutions was the square planar Rh^I anion $[Rh(CO)_2I_2]^-$ (**A**).[9] The overall rate of carbonylation showed a first-order dependence on the concentrations of both rhodium and iodide promoter. On the basis of these two observations, the reaction of **A** with MeI has been proposed to be the rate-determining step of the catalytic cycle.

Scheme I. Cycle for the Rhodium- and Iodide-Catalyzed Carbonylation of Methanol to Acetic Acid[5]

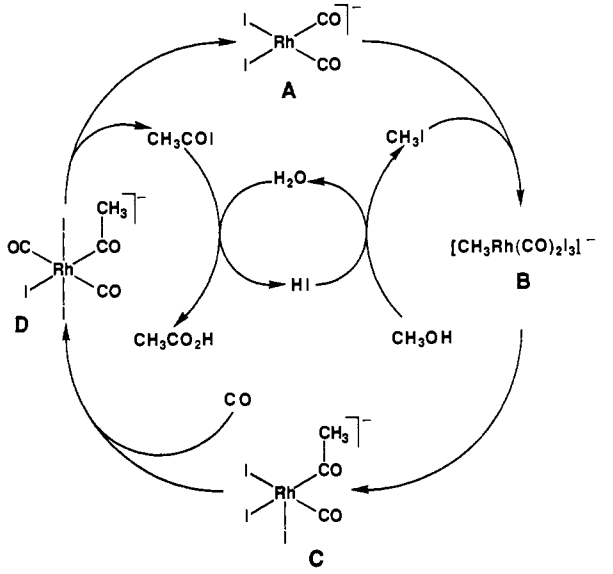

This oxidative addition reaction is believed to occur via nucleophilic attack by the rhodium center at the carbon of methyl iodide.[5]

In the previous studies of the reaction of **A** with MeI, the only product observed was the rhodium acyl complex **C**.[10] The intermediate rhodium methyl complex **B** was not detected, leading to the suggestion that the migratory insertion reaction **B** → **C** is very rapid in this system. However, an alternative explanation

(1) (a) University of Sheffield. (b) BP Chemicals, Hull.

(2) Collman, J. P.; Hegedus, L. S.; Norton, J. R.; Finke, R. G. *Principles and Applications of Organotransition Metal Chemistry*; University Science Books: Mill Valley, CA, 1987.

(3) (a) Polichnowski, S. W. *J. Chem. Educ.* **1986**, *63*, 204. Agreda, V. H. *Chem. Tech.* **1988**, 250. (b) Zoeller, J. R.; Agreda, V. H.; Cook, S. L.; Lafferty, N. L.; Polichnowski, S. W.; Pond, D. M. *Catalysis Today* **1992**, *13*, 73.

(4) Paulik, F. E.; Roth, J. F. *J. Chem. Soc., Chem. Commun.* **1968**, 1578. Roth, J. F.; Craddock, J. H.; Hershman, A.; Paulik, F. E. *Chem. Tech.* **1971**, 600.

(5) Forster, D. *Adv. Organomet. Chem.* **1979**, *17*, 255. Forster, D.; Singleton, T. C. *J. Mol. Catal.* **1982**, *17*, 299. Dekleva, T. W.; Forster, D. *Adv. Catal.* **1986**, *34*, 81.

(6) (a) Murphy, M.; Smith, B.; Torrence, G.; Aguilo, A. *Inorg. Chim. Acta.* **1985**, *101*, 147. (b) *J. Organomet. Chem.* **1986**, *303*, 257. (c) *J. Mol. Catal.* **1987**, *39*, 115.

(7) (a) Schrod, M.; Luft, G. *Ind. Eng. Chem. Prod. Res. Dev.* **1981**, *20*, 649. (b) Schrod, M.; Luft, G.; Grobe, J. *J. Mol. Catal.* **1983**, *20*, 175. (c) Lift, G.; Schrod, M. *J. Mol. Catal*, **1983**, *22*, 169.

(8) Hjortkjaer, J.; Jensen, V. W. *Ind. Eng. Chem. Prod. Res. Dev.* **1976**, *15*, 46. Hjortkjaer, J.; Jensen, O. R. *Ind. Eng. Chem. Prod. Res. Dev.* **1977**, *16*, 281. Hjortkjaer, J.; Jorgensen, J. C. A. *J. Mol. Catal.* **1978**, *4*, 199.

(9) Forster, D. *J. Am. Chem. Soc.* **1976**, *98*, 846.

(10) The X-ray structure determination shows **C** to be dinuclear in the solid state with six-coordinate Rh(III) and bridging iodides: Adamson, G. W.; Daly, J. J.; Forster, D. *J. Organomet. Chem.* **1974**, *71*, C17.

0002-7863/93/1515-4093$04.00/0

Scheme II. Kinetic Scheme for the Reaction of $[Rh(CO)_2I_2]^-$ with MeI

$$[Rh(CO)_2I_2]^- + MeI \underset{k_{-1}}{\overset{k_1}{\rightleftharpoons}} [MeRh(CO)_2I_3]^- \underset{k_{-2}}{\overset{k_2}{\rightleftharpoons}} [Rh(CO)(COMe)I_3]^-$$

A B C

is that reductive elimination of MeI from **B** is facile, leading to a rapid pre-equilibrium step, followed by rate-determining migratory insertion.

This paper describes how spectroscopically detectable quantities of **B** can be generated in the reaction of **A** with MeI, by using neat MeI as the reaction solvent. Using this approach, we have been able to characterize **B** using FTIR and low-temperature ^{13}C NMR spectroscopy, coupled with ^{13}C isotopic labeling. As a result of the detection of **B**, it has been possible to obtain reactivity data for this important catalytic intermediate and to distinguish between the two alternative explanations for its high reactivity. A preliminary account of some of this work has already been published.[11] Our conclusions are supported by new kinetic data on the solution behavior of specifically labeled $[Rh(^{12}CO)(^{13}COMe)I_3]^-$ (**C'**). We also report parallel results on the reaction of $[Rh(CO)_2Cl_2]^-$ with MeI, providing evidence for mixed halide rhodium methyl intermediates, $[MeRh(CO)_2Cl_nI_{3-n}]^-$.

Experimental Section

All operations were carried out under dry nitrogen. Methyl iodide and dichloromethane were distilled under nitrogen from calcium hydride. The rhodium complexes $[Bu_4N][Rh(CO)_2I_2]$, $[Bu_4N][Rh(CO)_2Cl_2]$, and $[Bu_4N][Rh(CO)(COMe)I_3]$ were prepared using synthetic procedures which have been described elsewhere.[12,13] Solutions of isotopically labeled $[Bu_4N][Rh(CO)_2X_2]$ (X = I, Cl) were prepared in situ for spectroscopic experiments by the reaction of a stoichiometric quantity of Bu_4NX with ca. 70% ^{13}CO-enriched $[Rh(CO)_2X]_2$. This method was used to prevent loss of isotopic label during isolation of the salts which necessitates the use of a CO atmosphere. The procedure used for ^{13}CO enrichment of $[Rh(CO)_2X]_2$ has been described elsewhere.[14] Specific ^{13}CO-labeling of the acyl carbonyl of $[Bu_4N][Rh(CO)(COMe)I_3]$ was achieved as follows. Reaction of $[Bu_4N][Rh(^*CO)_2I_2]$ (ca. 70% ^{13}CO enriched) with MeI gave $[Bu_4N][Rh(^*CO)(^*COMe)I_3]$, labeled to an equal extent in both terminal and acyl carbonyl positions. Repeated treatments with ^{12}CO, followed by N_2 purge, reduced the ^{13}CO content of the terminal carbonyl position to <5%, without significantly affecting the degree of labeling in the acyl group.

Kinetic Experiments. The reaction of $[Bu_4N][Rh(CO)_2I_2]$ with methyl iodide was monitored using FTIR spectroscopy in a solution cell (CaF_2 windows, 0.5-mm path length) fitted with a thermostatted jacket. IR spectra (2- or 4-cm^{-1} resolution) were recorded on a Perkin-Elmer 1710 Fourier Transform spectrometer and stored electronically using a PE 3600 data station. The collection, storage, and analysis of IR spectral data was automated using the OBEY programming language of the PE 3600 computer. Thus, a series of spectra could be collected with a constant time interval and stored to disk for subsequent analysis. Data processing involved subtraction of the solvent spectrum and extraction of absorbance data for the IR frequency of interest, giving a data set of absorbance against time for each kinetic run. Kinetic measurements were made by following the decay of the low-frequency ν(CO) absorption of $[Rh(CO)_2I_2]^-$ (1985 cm^{-1} in neat MeI). The pseudo-first-order rate constants (k_f) were found from the gradient of a plot of $\ln(Abs_0/Abs_t)$ against time, where Abs_0 is the initial absorbance and Abs_t the absorbance at time t. Good straight-line fits were obtained for these plots (correlation coefficient ≥ 0.999).

The concentration of $[Bu_4N][Rh(CO)_2I_2]$ used for IR spectroscopic measurements in neat MeI was typically 0.017 M. For analysis of the initial kinetic behavior of the weak bands of **B** and **C**, a rhodium concentration of 0.1 M was used.

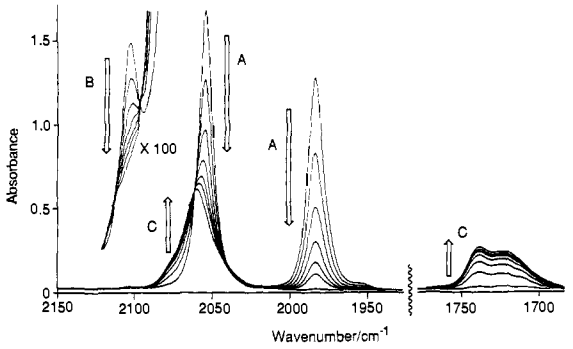

Figure 1. Series of IR spectra (ν(CO) region) illustrating the reaction of $[Bu_4N][Rh(CO)_2I_2]$ with neat MeI at 25 °C. The arrows indicate the behavior of each band as the reaction progresses. Note that the weak high-frequency absorption (expanded 100 times) due to intermediate rhodium methyl species, $[MeRh(CO)_2I_3]^-$ (**B**), decays at the same rate as those due the starting complex, $[Rh(CO)_2I_2]^-$ (**A**). The bands of the product, $[Rh(CO)(COMe)I_3]^-$ (**C**), are broad and shouldered due to the presence of a mixture of isomers.

^{13}C NMR Spectroscopy. ^{13}C NMR spectra were recorded using a Bruker WH400 spectrometer. When CH_3I or $^{13}CH_3I$ was used as solvent for NMR experiments, a small amount of acetone-d_6 (5–10% v/v) was added to provide the lock signal. Separate tests showed that the acetone had no effect on our measurements. For ^{13}C NMR experiments, the rhodium concentration was typically 0.2 M.

Warning: Methyl iodide is volatile and extremely toxic, and should only be used in an efficient fume hood or in a sealed cell.

Results

Kinetic Analysis. These studies are based on the kinetic analysis shown in Scheme II. Applying the steady-state approximation to the intermediate **B**, with the assumption that k_{-2} is small,[15] leads to the following relationship between the concentrations of **A** and **B**:

$$\frac{[B]}{[A]} = \frac{k_1[MeI]}{k_{-1} + k_2} \qquad (1)$$

A small relative concentration of **B** would therefore be expected when $(k_{-1} + k_2) \gg k_1[MeI]$, arising from either of the following two limiting situations: (i) rate-determining oxidative addition followed by rapid migratory insertion (i.e. large k_2, leading to $[B]/[A] \approx (k_1/k_2)[MeI]$); (ii) a rapid pre-equilibrium followed by rate-determining migratory insertion (i.e. large k_{-1}, leading to $[B]/[A] \approx (k_1/k_{-1})[MeI]$).

It is predicted that the steady-state concentration of **B** is directly proportional to the concentration of methyl iodide. We have therefore carried out experiments using neat methyl iodide as both reactant and solvent in order to generate detectable amounts of the intermediate. For other systems it has been found that rates of migratory insertion are slowed down by factors of more than 10^4 in nonpolar solvents.[16] Our use of a reaction medium of relatively low polarity should, therefore, favor accumulation of **B** by reducing the magnitude of k_2.

IR Spectroscopy of $[Bu_4N][Rh(CO)_2I_2]$ at High MeI Concentration. IR spectroscopy provides a sensitive tool for monitoring the reaction between $[Rh(CO)_2I_2]^-$ and MeI due to the relatively intense ν(CO) absorptions of the rhodium carbonyl species involved. Figure 1 illustrates the spectroscopic changes which were observed during the reaction of $[Bu_4N][Rh(CO)_2I_2]$ with neat MeI at 25 °C. The two terminal ν(CO) bands of **A** at 2055

(11) Haynes, A.; Mann, B. E.; Gulliver, D. J.; Morris, G. E.; Maitlis, P. M. *J. Am. Chem. Soc.* **1991**, *113*, 8567.
(12) Fulford, A.; Hickey, C. E.; Maitlis, P. M. *J. Organomet. Chem.* **1990**, *398*, 311.
(13) Fulford, A.; Bailey, N. A.; Adams, H.; Maitlis, P. M. *J. Organomet. Chem.* **1991**, *417*, 139.
(14) Adams, H.; Bailey, N. A.; Mann, B. E.; Manuel, C. P.; Spencer, C. M.; Kent, A. G. *J. Chem. Soc., Dalton Trans.* **1988**, 489.

(15) It can be assumed that $k_{-1}k_{-2}$ is small compared with $k_1k_2[MeI]$ when a high concentration of MeI is used, since the reaction A → C reaches completion under these conditions. The assumption is verified by quantitative measurements of k_{-1} and k_{-2} (see text).
(16) See, for example: Mawby, R.; Basolo, F.; Pearson, R. G. *J. Am. Chem. Soc.* **1964**, *86*, 3994. Butler, I. S.; Basolo, F.; Pearson, R. G. *Inorg. Chem.* **1967**, *6*, 2077.

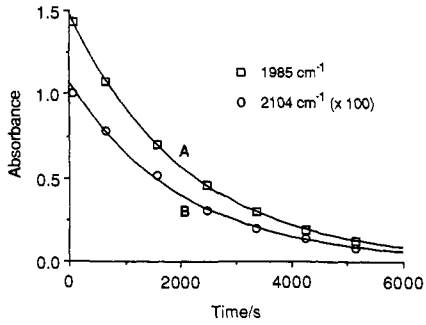

Figure 2. Plots of IR absorbance against time illustrating the kinetic behavior of absorptions due to $[Rh(CO)_2I_2]^-$ (**A**, 1985 cm^{-1}) and $[MeRh(CO)_2I_3]^-$ (**B**, 2104 cm^{-1}, expanded 100 times) during the reaction of $[Bu_4N][Rh(CO)_2I_2]$ with neat MeI at 25 °C. The best exponential decays fitted to each set of data points are also shown. Note that both absorptions decay at the same rate, in accordance with the predictions of the steady-state approximation.

Table I. IR Spectroscopic Data for Rhodium Complexes Observed in This Work and Data for Analogous Iridium Complexes for Comparison

complex	ν(CO)/cm^{-1} (CH_2Cl_2)	ν(CO)/cm^{-1} (MeI)
$[Rh(^{12}CO)_2I_2]^-$ (**A**)	2059, 1988	2055, 1985
$[Rh(^{12}CO)(^{13}CO)I_2]^-$ (**A'**)	2041, 1958	2037, 1953
$[Rh(^{13}CO)_2I_2]^-$ (**A''**)	2011, 1943	2006, 1939
$[Rh(CO)_2Cl_2]^-$	2069, 1992	2064, 1987
$[MeRh(CO)_2I_3]^-$ (**B**)		2104, 2060 ± 3[a]
$[MeRh(^{12}CO)(^{13}CO)I_3]^-$ (**B'**)		2090, 2023 ± 6[b]
$[MeRh(CO)_2Cl_2I]^-$		2121
$[Rh(^{12}CO)(^{12}COMe)I_3]^-$ (**C**)	2065, 1737	2061, 1740
$[Rh(^{12}CO)(^{13}COMe)I_3]^-$ (**C'**)	2065, 1698	2061, 1704
$[Rh(^{13}CO)(^{12}COMe)I_3]^-$ (**C''**)	2017, 1737	2014, 1740
$[Ir(CO)_2I_2]^-$	2046, 1968	
$[Ir(CO)_2Cl_2]^-$	2054, 1971	
$[MeIr(CO)_2I_3]^-$	2098, 2045	
$[MeIr(CO)_2Cl_2I]^-$	2111, 2055	

[a] Low-frequency ν(CO) of **B** resolved by computer subtraction of intense bands of **A** and **C**. [b] Calculated low-frequency ν(CO) of **B'** based on isotopic labeling studies—see text.

and 1985 cm^{-1} were replaced by the terminal and acyl ν(CO) absorptions of **C** at 2061 and 1740 cm^{-1}, respectively. The spectrum of the product, **C**, exhibits quite broad absorptions with shoulders, which are due to the presence of a mixture of isomers.[14]

Careful inspection of these IR spectra revealed the presence of a much weaker absorption at 2104 cm^{-1}, which was not present for solutions of either **A** or **C** in other solvents. This band does not correspond to any known rhodium carbonyl iodide species which might be formed as a byproduct, such as *cis*- or *trans*-$[Rh(CO)_2I_4]^-$. The kinetic traces in Figure 2 show that during the reaction the weak absorption decays in direct proportion to the band due to **A** at 1985 cm^{-1}. The ratio of the two absorbances, R_{Abs} (= Abs_{2104}/Abs_{1985}), was found to be directly proportional to [MeI] over the range 12–16 M in CH_2Cl_2 at 25 °C. According to the Beer–Lambert law, R_{Abs} is directly proportional to the ratio of concentrations of the species responsible for the two absorptions. Therefore, the absorption at 2104 cm^{-1} behaved exactly as predicted for a ν(CO) mode of **B** by the steady-state approximation (eq 1).

The IR spectrum of a dicarbonyl complex, such as **B**, is expected to exhibit two ν(CO) absorptions. An excellent model is provided by the analogous iridium system, in which oxidative addition of MeI to $[Ir(CO)_2I_2]^-$ yields $[MeIr(CO)_2I_3]^-$, which is stable under ambient conditions. On the basis of IR data for these iridium species (Table I), the low-frequency ν(CO) band of **B** is expected to occur very close to the high-frequency ν(CO) band of **A**. Further detailed IR spectroscopic studies have now allowed resolution of the low-frequency ν(CO) band of **B**.

A series of IR spectra were obtained during the first few minutes of the reaction of **A** with neat MeI at 5 °C. Under these conditions, it is possible to monitor the initial growth of the ν(CO) band of **B** at 2104 cm^{-1} to its steady-state value.[11] IR difference spectra, generated by computer subtraction of the first spectrum of the series from subsequent spectra, exhibit negative absorptions at 2055 and 1985 cm^{-1} due to loss of **A** and positive absorptions at 2104, ca. 2060, and 1740 cm^{-1} due to the formation of **B** and **C**. However, the positive band at ca. 2060 cm^{-1} is too intense relative to that at 1740 cm^{-1} to be wholly accounted for by the terminal ν(CO) band of **C**, suggesting the contribution of another absorption at this frequency. Indeed, scaled computer subtraction of the absorptions of **A** and **C** reveals a band at ca. 2060 cm^{-1}, which displays similar intensity and identical kinetic behavior to that at 2104 cm^{-1}. Both of these weak absorptions can, therefore, be assigned to the intermediate, **B**.

IR Spectroscopy of ^{13}CO-Enriched $[Bu_4N][Rh(CO)_2I_2]$ in MeI. Additional IR spectroscopic measurements have been made, using ^{13}CO-enriched samples of **A**, in order to confirm assignment of these weak absorptions to an intermediate dicarbonyl species. When the reaction of ca. 70% ^{13}CO-enriched $[Bu_4N][Rh(CO)_2I_2]$ with neat MeI was monitored using FTIR spectroscopy, a weak absorption was observed at 2090 cm^{-1}, which exhibited kinetic behavior identical to that of the bands observed without isotopic labeling. This band can therefore be assigned to an isotopomer of the same complex. The frequency shift which occurs on isotopic substitution provides information about the number of carbonyl ligands present. Substitution of a monocarbonyl species by ^{13}CO is expected to cause a relatively large shift of ν(CO) to lower frequency of ca. 48 cm^{-1}. The shift of 14 cm^{-1} observed here is consistent with that expected for a dicarbonyl complex, the bands at 2104 and 2090 cm^{-1} being assigned to the high-frequency ν(CO) modes of $M(^{12}CO)_2$ and $M(^{12}CO)(^{13}CO)$ moieties, respectively.[17]

Observation of these two frequencies allows calculation of the two CO factored force constants of the $M(CO)_2$ unit, and hence the frequencies of other ν(CO) bands can be estimated. Using this method, the low-frequency band of the $M(^{12}CO)_2$ species is predicted to occur at 2057 ± 6 cm^{-1}.[18] This is in excellent agreement with our assignment of a weak band observed at ca. 2060 cm^{-1} as the low frequency band of **B** (see above).

Thus, the intermediate observed by FTIR spectroscopy has two ν(CO) bands which are shifted to high frequency relative to those of **A**. This shift indicates a decrease of electron density at the rhodium center and is characteristic of an oxidative addition reaction. Very similar shifts in ν(CO) occur in the analogous iridium system (Table I), supporting our assignment of weak IR bands to the oxidative addition product, $[MeRh(CO)_2I_3]^-$ (**B**).

Low-Temperature ^{13}C NMR Spectroscopy of $[Bu_4N][Rh(CO)_2I_2]$ in MeI. The reaction of **A** with MeI has also been monitored using high-resolution, low-temperature ^{13}C NMR spectroscopy. The IR band intensities indicate that the steady-state concentration of **B** is only ca. 1% of that of the starting rhodium complex (**A**). We have therefore carried out experiments using ^{13}C enrichment in both methyl and carbonyl positions. A high concentration of MeI was again used to generate a large relative concentration of the intermediate species. Even under these favorable conditions, it was necessary to accumulate many scans in order to resolve weak signals due to species at low concentration. Therefore samples were made up at low temperature (ca. −50 °C) and only briefly warmed to room temperature to allow the reaction to proceed. Spectra were recorded after cooling back to −50 °C, which effectively stopped the reaction.

(17) Braterman, P. S. *Metal Carbonyl Spectra*; Academic Press: London, 1975.

(18) The parameters used in this prediction were C–O stretching force constant k = 1748 ± 5 N m^{-1} and the interaction force constant i = 40 ± 5 N m^{-1}. Quite large errors arise from the uncertainty (ca. ±0.5 cm^{-1}) in the measurement of the peak position of weak bands of **B**. Our treatment assumes equivalent carbonyl ligands, as supported by NMR data.

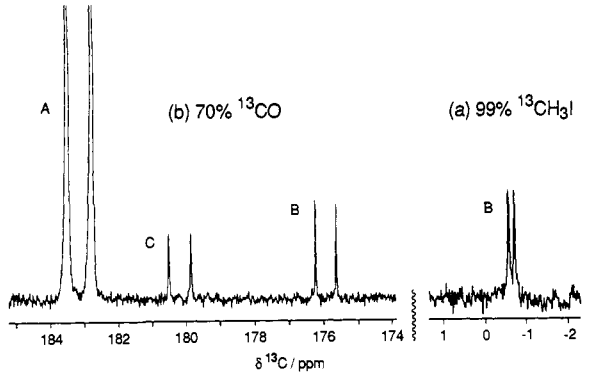

Figure 3. Low-temperature ^{13}C NMR spectra (−50 °C) illustrating the reaction of $[Bu_4N][Rh(CO)_2I_2]$ with MeI. The spectra were recorded in two different experiments: (a) rhodium methyl region, using 99% ^{13}C-enriched MeI and (b) terminal rhodium carbonyl region, using ca. 70% ^{13}CO-enriched rhodium complex. The signal of **A** is off scale due to the large expansion. Resonances are labeled according to their assignment. All the signals are doublets due to ^{103}Rh–^{13}C coupling.

In one experiment, a solution of $[Bu_4N][Rh(CO)_2I_2]$ in $^{13}CH_3I$ (containing 5% v/v $(CD_3)_2CO$ for the NMR lock signal) was made up at −50 °C and quickly transferred to the probe of the NMR spectrometer at −50 °C. The initial low-temperature ^{13}C-{^{1}H} NMR spectrum of this sample showed signals arising from natural abundance ^{13}C in the starting rhodium complex as well as the very strong signal of $^{13}CH_3I$ at −19.7 ppm and several very weak signals due to nonreacting trace impurities in the $^{13}CH_3I$.[19]

The spectrum, shown in Figure 3a, recorded after brief warming of the sample to room temperature, showed a weak new doublet at δ −0.65 ppm, in the region characteristic of a rhodium methyl, with splitting (J = 14.7 Hz) consistent with $^1J(^{103}Rh–^{13}C)$ coupling (^{103}Rh, 100%, $I = {}^1/_2$). Signals were also observed due to a small amount of the rhodium acyl complex, **C** (δ 48.44 and 49.78 ppm, arising from the methyls of two isomers). When the spectrum of the same sample was recorded without ^{1}H-decoupling, the rhodium methyl signal was split into a quartet of doublets, with $^1J(^{13}C–^1H)$ = 143 Hz, identical to that found for the methyl group in $[CH_3Rh(PPh_3)_2I_2]$.[20]

The ^{1}H chemical shift (δ 2.08 ppm) of the methyl protons of **B** was determined indirectly from the ^{13}C NMR spectrum, using off-resonance decoupling.[21] This is again typical of a rhodium methyl species. Direct observation of this signal by ^{1}H NMR spectroscopy was impossible, due to the proximity of the intense resonance of $^{13}CH_3I$ at δ 2.22 ppm.

A similar experiment was performed using ca. 70% ^{13}CO-enriched $[Bu_4N][Rh(CO)_2I_2]$ in enriched MeI. The initial low-temperature spectrum showed a single intense doublet in the rhodium carbonyl region (δ 183.2, $^1J(^{103}Rh–^{13}C)$ = 72.3 Hz), due to **A**.[22] The spectrum shown in Figure 3b was recorded after brief warming of the sample to room temperature and contains two new much weaker rhodium carbonyl signals. The doublet centered at δ 180.2 ($^1J(^{103}Rh–^{13}C)$ = 66.1 Hz) is due to the terminal carbonyl of the rhodium acyl complex, **C**. A signal due to the acyl carbonyl of **C** was also located (Table II). The other weak doublet in the terminal carbonyl region (δ 175.9 ppm ($^1J(^{103}Rh–^{13}C)$ = 59.9 Hz)) is assigned to the intermediate, **B**. The carbonyl ^{13}C resonance of **B** is shifted to high field relative to that of **A**, as found for the corresponding conversion in the iridium system (Table II). The relative ^{13}C intensities for the carbonyls of **A** and **B** suggest that the concentration of **B** is ca. 1% that of **A**, in agreement with the IR data.

Table II. ^{13}C NMR Spectroscopic Data for Rhodium Complexes Observed in This Work (Solvent: MeI + 5% Acetone-d_6) and Data for Analogous Iridium Complexes for Comparison (Solvent: CD_2Cl_2)

complex	δ ^{13}C/ppm	$^1J(^{103}Rh–^{13}C)$/Hz
$[Rh(CO)_2I_2]^-$ (**A**)	183.2	72.3
$[Rh(CO)_2Cl_2]^-$	181.5	71.2
$[Rh(CO)_2ClI]^-$	180.9 (*C*O trans to Cl)	74.8
	182.7 (*C*O trans to I)	68.1
$[MeRh(CO)_2I_3]^-$ (**B**)	175.9 (*C*O)	59.9
	−0.65 (*C*H$_3$)	14.7
$[MeRh(CO)_2Cl_nI_{3-n}]^-$	177.7, 173.3 (*C*O)	60.3, 59.2
	5.75 (*C*H$_3$)	14.6
$[Rh(CO)(COMe)I_3]^-$ (**C**)	207.3 (*C*OCH$_3$)	22.5
	180.2 (*C*O)	66.1
	48.44, 49.78 (CO*C*H$_3$)	
$[Ir(CO)_2I_2]^-$	169.7 (*C*O)	
$[Ir(CO)_2Cl_2]^-$	167.8 (*C*O)	
$[MeIr(CO)_2I_3]^-$	155.5 (*C*O)	
	−16.3 (*C*H$_3$)	
$[MeIr(CO)_2Cl_2I]^-$	157.5 (*C*O)	
(Me trans to I)	−3.1 (*C*H$_3$)	
$[MeIr(CO)_2Cl_2I]^-$	158, 155 (*C*O)	
(Me trans to Cl)	−9.5 (*C*H$_3$)	

On allowing the reaction of **A** with MeI to reach completion, the methyl and carbonyl ^{13}C signals assigned to **B** could no longer be detected, as expected for an intermediate species. When ^{13}C-enriched samples of both **A** and MeI were used, both the methyl and carbonyl ^{13}C resonances of **B** could be observed for the same sample. However, no coupling between the methyl and carbonyl resonances was detected.

Structure of $[MeRh(CO)_2I_3]^-$ (B). Three alternative structures for a complex with the formula $[MeRh(CO)_2I_3]^-$ are illustrated below, two possessing cis dicarbonyl geometry and one having a trans dicarbonyl configuration.

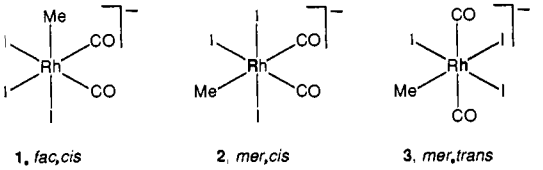

1, *fac,cis* 2, *mer,cis* 3, *mer,trans*

The ^{13}C NMR spectrum of **B** has only one doublet in the rhodium carbonyl region, indicative of equivalent carbonyl ligands, consistent with either structure **1** or **3** but not **2**. Further, no coupling was observed between the methyl and carbonyl carbons in **B**, which is also consistent with structure **1** or **3**, since a very small value of $^2J(^{13}C–^{13}C)$ is expected for methyl cis to carbonyl.

The IR spectra of **1** and **3** are both predicted to exhibit two ν(CO) absorptions. For a cis dicarbonyl complex, such as **1**, the two bands are expected to have similar intensities, whereas for a trans dicarbonyl, such as **3**, the high-frequency (symmetric) ν(CO) mode is expected to be much weaker than the low-frequency (antisymmetric) mode.[23] In the IR spectroscopic studies described above, two ν(CO) bands of similar intensity were observed, which

(19) The ^{13}C NMR spectrum of the $^{13}CH_3I$ used in this work showed several very weak doublets and higher multiplets with coupling constants of ca. 35 Hz, consistent with $^1J(^{13}C–^{13}C)$. These signals, which remained unchanged throughout each experiment, are assigned to highly ^{13}C-enriched longer chain alkyl halides.

(20) Siedle, A. R.; Newmark, R. A.; Pignolet, L. H. *Organometallics* **1984**, *3*, 855.

(21) In this technique, the splitting of the ^{13}C resonance due to C–H coupling is monitored as a function of specific low-power decoupling frequency, enabling the resonant frequency of protons bonded to the carbon of interest to be determined. This technique is much faster than 2-D ^{13}C–^{1}H correlation for a single methyl group: Archer, R. A.; Cooper, R. D. G.; Demarco, P. V.; Johnson, L. R. F. *J. Chem. Soc., Chem. Commun.* **1970**, 1291. Wehrli, F. W.; Wirthlin, T. *Interpretation of Carbon-13 NMR spectra*; Heyden: London, 1978; p 69.

(22) Brown, C.; Heaton, B. T.; Longhetti, L.; Povey, W. T.; South, D. O. *J. Organomet. Chem.* **1980**, *192*, 93.

(23) For example, in the trans dicarbonyl complex, $[Rh(CO)_2(COMe)I_3]^-$, the ratio of ν(CO) intensities is $Abs_{2141}/Abs_{2084} \approx 1/20$.

Table III. Kinetic and IR Absorbance Ratio Data Measured in This Study

T/°C	$10^4k_f{}^b$/s^{-1}	$10^3R_{Abs}{}^c$	$10^3k_2{}^d$/s^{-1}	$10^5k_{-2}{}^e$/s^{-1}
5	1.09	10.5	8.3	
15	2.24	8.4	21	0.263
25	4.69	7.0	54	1.03
35	9.78	5.9	133	4.20

[a] Estimated errors in rate constants are ±2% in k_f, ±10% in k_2 (due to uncertainty in R_ϵ), and ±5% in k_{-2}. [b] k_f is the observed pseudo-first-order rate constant for the conversion of **A** into **C** in neat MeI. [c] R_{Abs} is the ratio of IR intensities of bands due to complexes **B** and **A**, Abs_{2104}/Abs_{1985}. [d] The first-order rate constant for migratory insertion (**B** → **C**); calculated from k_f and R_{Abs} as described in the text with an estimate of $R_\epsilon = 0.8$. [e] k_{-2} is the first-order rate constant for deinsertion (**C** → **B**).

can be assigned to **B**. We therefore strongly favor the cis dicarbonyl structure, **1**; this geometry has indeed been observed for the iridium analog.[24]

Our spectroscopic studies do not give direct information about the number of iodide ligands in **B**. An alternative formulation for the intermediate we have observed is a neutral five-coordinate complex, $[MeRh(CO)_2I_2]$. This would be the initial product of a two-step oxidative addition process involving nucleophilic attack of **A** on MeI. Such a species should be converted into the anionic, six-coordinate $[MeRh(CO)_2I_3]^-$ at high iodide concentration. However, when an excess of iodide was added to solutions of **B**, only minute changes, consistent with medium effects, were observed in both the IR and ^{13}C NMR spectra of **B**.[25] In the analogous iridium system, there is a considerable shift of ca. 25 cm^{-1} between the ν(CO) bands of $[MeIr(CO)_2I_3]^-$ and $[MeIr(CO)_2I_2]$. The spectroscopic data therefore suggest that **B** has the formula $[MeRh(CO)_2I_3]^-$ and are consistent with structure **1**. However, it is possible that in more coordinating solvents, such as methanol, substitution of I^- might give a neutral solvento complex, $[MeRh(CO)_2I_2(solvent)]$.

Kinetic Behavior of $[MeRh(CO)_2I_3]^-$ (B). The kinetic behavior of **B** has been monitored using FTIR spectroscopy, allowing reactivity data for the intermediate to be obtained. At high MeI concentrations, pseudo-first-order conditions apply and the observed rate constant (k_f) for the conversion of **A** into **C** is given by

$$k_f = \frac{k_1k_2[MeI]}{k_{-1} + k_2} \qquad (2)$$

Combining this expression with that derived for [B]/[A] (eq 1) gives

$$k_2 = k_f\frac{[A]}{[B]} = k_f\frac{R_\epsilon}{R_{Abs}}$$

where R_{Abs} has already been defined as Abs_{2104}/Abs_{1985} and R_ϵ is the corresponding ratio of extinction coefficients for these bands, $\epsilon_{2104}/\epsilon_{1985}$. Both k_f and R_{Abs} can be measured directly by IR spectroscopy. Therefore, an estimate of R_ϵ allows us to obtain a value for k_2.[26] Experimentally determined values of k_f and R_{Abs} and derived values of k_2 over the range 5–35 °C are given in Table III. An Arrhenius plot of the k_2 data is a good straight line (correlation coefficient 0.999), yielding the activation parameters given in Table IV.[27]

Table IV. Activation Parameters for the Overall Reaction of **A** with Neat **MeI**, Migratory Insertion in **B** (Neat MeI), and Deinsertion in **C** (3.2 M MeI in CH_2Cl_2)

reaction (rate constant)	**A** + MeI → **C** (k_f/MeI)	**B** → **C** (k_2)	**C** → **B** (k_{-2})
$\Delta H^\ddagger$/kJ mol^{-1}	50 ± 1	63 ± 2	100 ± 1
$\Delta S^\ddagger$/J mol^{-1} K^{-1}	−165 ± 4	−59 ± 9	−5 ± 4
$\Delta G^\ddagger_{298}$/kJ mol^{-1}	99 ± 1	81 ± 2	101 ± 1

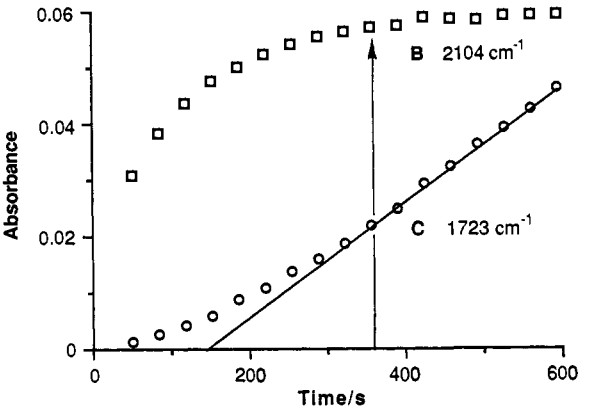

Figure 4. Plots of IR absorbance against time showing the behavior of the bands due to **B** (2104 cm^{-1}) and **C** (1723 cm^{-1}) in the first 10 min of the reaction of $[Bu_4N][Rh(CO)_2I_2]$ (0.1 M) with neat CH_3I at 5 °C. The straight-line fit for the 1723-cm^{-1} data between 6 and 10 min indicates the maximum rate of formation of **C**. Note that this rate is achieved at the same time as the concentration of **B** reaches its peak (indicated by the arrow).

In all the kinetic experiments described above, the intermediate **B** was observed at its steady-state concentration, such that the ratio [B]/[A] remained constant throughout the reaction. However, the steady-state approximation does not hold in the very early stages of the reaction, since there must be a finite time after mixing the reactants in which the ratio [B]/[A] grows from zero to its steady-state value. This "relaxation time" was too fast to measure using conventional techniques at 25 °C or above, but by monitoring the reaction below ambient temperature, we were able to observe the initial appearance of the IR band due to **B**.

Figure 4 shows kinetic plots for the absorptions of both **B** and **C** during the first few minutes of the reaction at 5 °C. The 2104-cm^{-1} absorption, assigned to **B**, does not attain its maximum intensity until ca. 6 min after mixing. Thereafter, the absorption decays at the same rate as that of **A** at 1985 cm^{-1}. In addition, the rate of formation of **C** (given by the slope of the plot of Abs_{1723} against time) reaches its maximum at the same time as the band at 2104 cm^{-1} attains its peak intensity. Thus the rate of product formation is proportional to the concentration of the intermediate species. The attainment of steady-state behavior at the start of the reaction in this system should approximate to a first-order process with a rate constant of $(k_1[MeI] + k_{-1} + k_2)$. Since $(k_{-1} + k_2) \gg k_1[MeI]$ (see Kinetic Analysis, above), this expression can be further simplified to $(k_{-1} + k_2)$. We were able to measure a first-order rate constant of $(8.5 \pm 0.2) \times 10^{-3}$ s^{-1} for this process at 5 °C. This value is very close to that obtained for k_2 at the same temperature (Table III), suggesting that the term $(k_{-1} + k_2)$ is dominated by k_2 under these conditions.

Solution Behavior of $[Rh(^{12}CO)(^{13}COMe)I_3]^-$ (C′) in CH_2Cl_2. It was noted by Forster[9] that **C** degrades to give **A** at 200 °C, suggesting that both oxidative addition and migratory insertion are reversible (Scheme II). Similarly, we have observed that **A**

(24) There are no X-ray crystallographic data for $[MeIr(CO)_2I_3]^-$, but spectroscopic data are consistent with fac,cis stereochemistry, analogous to structure **1**. The closely related neutral dinuclear complex $[MeIr(CO)_2Cl_2]_2$ is also known to contain *fac*-$MeIr(CO)_2$ units: Bailey, N. A.; Jones, C. J.; Shaw, B. L.; Singleton, E. *J. Chem. Soc., Chem. Commun.* **1967**, 1051.

(25) The shifts observed for spectroscopic features of **B** at 0.2 M Bu_4NI were ca. 1 cm^{-1} (ν(CO)), 0.2 ppm ($\delta(^{13}CH_3)$), and 0.1 ppm ($\delta(^{13}CO)$).

(26) We have used an estimated value of $R_\epsilon = 0.8$ in our calculation of k_2. This is based on both the initial changes in IR absorbance at 2104 and 1985 cm^{-1} observed at 5 °C and comparison of relative band intensities for model systems such as $[Ir(CO)_2I_2]^-$/$[MeIr(CO)_2I_3]^-$ and $[Rh(CO)_2I_2]$ /*cis*-$[Rh(CO)_2I_4]^-$. This is a slight modification of the estimate of $R_\epsilon = 0.7$ in the preliminary account of this work.[11]

(27) The margin of error quoted for $\Delta S^\ddagger$ takes into account the uncertainty in our estimate of R_ϵ, which affects the intercept but not the slope of the Arrhenius plot.

Scheme III. Possible Reactions for the Isotopically Enriched Complex, $[Rh(^{12}CO)(^{13}COMe)I_3]^-$ (C′) (The Rate Constants Are the Same as Those Defined in Scheme II.)

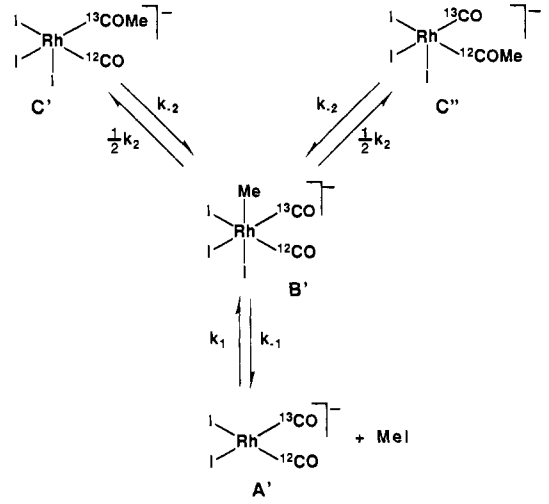

is formed slowly but quantitatively from solutions of C in CH_2Cl_2 at ambient temperature and that exchange of methyl groups occurs between C and $^{13}CH_3I$.[28] We have investigated the solution behavior of samples of C specifically labeled with ^{13}CO in the acyl carbonyl position, using FTIR spectroscopy. This has enabled us to determine k_{-2}, the rate constant for migratory deinsertion in C, and to evaluate k_2/k_{-1}, which defines the relative importance of the two modes of reaction for B.

The system of reactions possible for specifically ^{13}C-labeled $[Rh(^{12}CO)(^{13}COMe)I_3]^-$ (C′) is illustrated in Scheme III. Migration of methyl from carbonyl to rhodium in C′ gives a rhodium methyl species, B′, containing isotopically inequivalent carbonyls. There are three possible fates for this intermediate: (i) migration of methyl onto ^{13}CO (giving back C′), (ii) migration of methyl onto ^{12}CO (giving C″), (iii) reductive elimination of MeI (giving A′).

The NMR data indicate that the carbonyl ligands of B are chemically equivalent, so the two distinct migratory insertion steps (i) and (ii) are equally probable, assuming that isotope effects are negligible. If the migratory insertion step is reversible (i.e. $k_{-2} \neq 0$), the ^{13}CO label would be expected to become scrambled between acyl and terminal carbonyl positions in a first-order process with a rate constant of k_{-2}.

The solution behavior of C, containing ca. 70% ^{13}CO enrichment in the acyl ligand, was monitored at high [MeI] using IR spectroscopy; use of a high concentration of MeI suppresses reductive elimination (iii) and effectively isolates the methyl migration process. Identical results were obtained using either neat MeI or 3.2 M MeI in CH_2Cl_2 as the solvent. During the reaction, the terminal and acyl ν(CO) bands of $[Rh(^{12}CO)(^{13}COMe)I_3]^-$ (C′) decreased in intensity, and absorptions of the rearranged isotopomer $[Rh(^{13}CO)(^{12}COMe)I_3]^-$ (C″) appeared, showing that methyl migration between labeled and unlabeled carbonyls can occur in C.[29] Kinetic plots obtained in one of these experiments are shown in Figure 5. The exponential decay of the terminal $\nu(^{12}CO)$ absorption of C′ to a limiting value

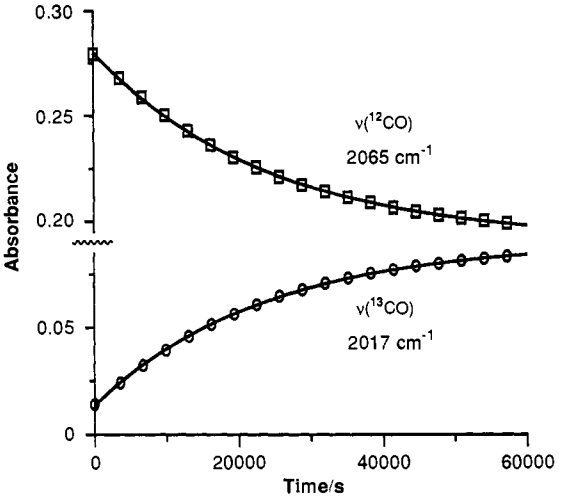

Figure 5. Plots of IR absorbance against time illustrating the solution behavior of $[Bu_4N][Rh(CO)(COMe)I_3]$ containing 70% enrichment in the acyl carbonyl position (3.2 M MeI, CH_2Cl_2, 35 °C). Note the decay of the terminal $\nu(^{12}CO)$ absorption at 2065 cm^{-1} and corresponding increase of the terminal $\nu(^{13}CO)$ absorption at 2017 cm^{-1} due to conversion of $[Rh(^{12}CO)(^{13}COMe)I_3]^-$ (C′) into $[Rh(^{13}CO)(^{12}COMe)I_3]^-$ (C″). The good exponential fits to the data show that the approach to a statistical distribution of isotopic label is a first-order process.

is exactly mirrored by the growth of the terminal $\nu(^{13}CO)$ absorption of C″. At equilibrium, a statistical distribution of the ^{13}CO label between terminal and acyl positions was attained. The rate of approach to equilibrium was found to be the same in both neat MeI and 3.2 M MeI in CH_2Cl_2. The rate of isotopic label scrambling in C′ has been studied over the range 15–35 °C, giving the values of k_{-2} shown in Table III. An Arrhenius plot constructed from these data gives activation parameters for the migratory deinsertion process C → B (Table IV).

The behavior of the same labeled starting material was also monitored in CH_2Cl_2 solution in the absence of added MeI. In this experiment, the conversion of C′ into C″ was accompanied by the production of another set of bands in the terminal ν(CO) region, due to A and A′ (see Table I). The formation of isotopomers of $[Rh(CO)_2I_2]^-$, via reductive elimination of MeI, is a much slower process than the scrambling of isotopic label between terminal and acyl carbonyl positions. We have obtained a first-order rate constant k_b for the process C → A + MeI of 4.05×10^{-6} s^{-1} at 35 °C in CH_2Cl_2.

Kinetic analysis of the mechanism shown in Scheme II leads to the expression

$$k_b = k_{-1}k_{-2}/(k_{-1} + k_2)$$

for conversion of C to A. Rearrangement gives

$$k_2/k_{-1} = (k_{-2}/k_b) - 1$$

Substituting the measured values of k_{-2} and k_b indicates that the ratio $k_2/k_{-1} \approx 9$ in CH_2Cl_2 at 35 °C. This, combined with the value of k_2 obtained in neat MeI at 35 °C (Table III), gives a value for k_{-1} of ca. 1.5×10^{-2} s^{-1} (35 °C).[30] These measurements confirm our conclusion that migratory insertion is fast relative to reductive elimination of MeI, based on the kinetic behavior observed for B (see above), and unambiguously establish that the previous nonobservation of B is primarily due to rapid migratory insertion.

Knowledge of the ratio k_2/k_{-1}, together with the rate constant for the overall reaction A + MeI → C (k_f, Table III), also enables accurate determination of the rate constant for oxidative addition k_1. In all previous studies of the reaction of A with MeI,[6,12] k_1 has been obtained using the approximation $k_1 = k_f/[MeI]$, with

(28) This reaction was followed by monitoring the ^1H resonances of C and MeI. A $^{12}CH_3$ moiety gives rise to a singlet, whereas a $^{13}CH_3$ group gives a doublet due to C–H coupling. Free $^{12}CH_3I$ and $[Rh(CO)(CO^{13}CH_3)I_3]^-$ were generated slowly at room temperature.

(29) During a previous study of the same system, using ^{13}C NMR spectroscopy, no evidence for methyl scrambling was obtained, but substantial decomposition of the sample was noted.[14] We have found that the rate of methyl scrambling is sensitive to the presence of ligands such as MeOH or H_2O which slow down the process. It is possible that such an impurity was present during the original studies. The present studies predict a half-life of ca. 40 h for methyl scrambling under the conditions of the original work (ca. 20 °C) rather than >150 h, as suggested by the original observations.

(30) This treatment assumes that k_2 is the same in CH_2Cl_2 as in MeI.

the assumption that k_{-1} was negligible compared to k_2. Using the ratio $k_2/k_{-1} = 9$, a value of k_1 (35 °C) = 6.8×10^{-5} M^{-1} s^{-1} is obtained. Thus, each of the four rate constants describing the reaction between **A** and MeI (Scheme II) has been determined at 35 °C.

Reaction of $[Rh(CO)_2Cl_2]^-$ with MeI: Detection of $[MeRh(CO)_2Cl_nI_{3-n}]^-$. We have previously reported that the reaction of MeI with $[Rh(CO)_2Cl_2]^-$ leads to halide exchange, giving **A** and MeCl, as well as the formation of rhodium acyl species.[13] IR spectroscopic evidence was obtained for an intermediate mixed halide complex, $[Rh(CO)_2ClI]^-$, but the complete mechanism of exchange was not elucidated. We now present evidence for the participation of rhodium methyl complexes in the exchange reaction, suggesting an oxidative addition/reductive elimination sequence.

When the reaction of $[Bu_4N][Rh(CO)_2Cl_2]$ with neat MeI was monitored using FTIR spectroscopy, a weak absorption was observed at 2121 cm^{-1}, somewhat higher frequency than that assigned to **B** in the reaction of **A** with MeI. Such a shift is characteristic of substitution of iodide by chloride in rhodium carbonyl halide complexes. At 5 °C, the weak absorption at 2121 cm^{-1} grew to its maximum intensity during the initial stages of the reaction, exactly as observed for **B**. This band is therefore assigned to the mixed halide complex, $[MeRh(CO)_2Cl_2I]^-$, the initial product of oxidative addition of MeI to $[Rh(CO)_2Cl_2]^-$.

The halide exchange between $[Rh(CO)_2Cl_2]^-$ and MeI can be followed by monitoring the shift in ν(CO) bands to lower frequency. As this reaction proceeded, the peak position of the weak absorption also moved slowly to lower frequency. When the formation of $[Rh(CO)_2I_2]^-$ was complete, the weak absorption had shifted to 2104 cm^{-1}, the same as that observed for **B**. The band subsequently decayed at the same rate as **A**, exactly as observed in the reaction of **A** with MeI.

Mixed halide rhodium methyl intermediates would be expected to undergo migratory insertion reactions in the same way as **B**, leading to a mixture of rhodium acyl complexes, $[Rh(CO)(COMe)Cl_nI_{3-n}]^-$ (n = 0–2). The broad, shouldered acyl ν(CO) absorption generated during the reaction between $[Rh(CO)_2Cl_2]^-$ and MeI displayed reproducible changes in band shape, which we ascribe to varying proportions of the chloro–iodo products. No corresponding variations in band shape were observed in the reaction of **A** with MeI. The presence of chloride ligand was confirmed by elemental analysis, which gave a value for the ratio I/Cl of ca. 6/1 for the product obtained from the reaction of $[Rh(CO)_2Cl_2]^-$ with neat MeI (4 h, 20 °C).

The reaction of $[Rh(CO)_2Cl_2]^-$ with MeI was also monitored at −50 °C by ^{13}C NMR spectroscopy, using ^{13}C-enriched reactants. After brief warming of the sample to room temperature to allow reaction to occur, several doublets were observed in the rhodium carbonyl region of the spectrum, the most intense of which was due to the parent rhodium complex. Three other relatively strong doublets are assigned to **A** and the inequivalent carbonyls of the mixed halide complex, $[Rh(CO)_2ClI]^-$, which has previously been observed only by IR spectroscopy.[13] The chemical shifts and $J(^{103}Rh-^{13}C)$ coupling constants for these species are given in Table II. Halide exchange is confirmed by the appearance of a resonance due to MeCl at δ 27.0. Three much weaker doublets were also apparent in the carbonyl region of the ^{13}C NMR spectrum. One of these, at δ 176.0 ($J(^{103}Rh-^{13}C)$ = 59.9 Hz), corresponds well with the signal assigned to **B**. The other two doublets have very similar coupling constants and can be assigned either to inequivalent carbonyls in a mixed halide rhodium methyl complex or to two carbonyls of different complexes.

In the rhodium methyl region of the spectrum, doublets were generated at δ −0.65 (J = 14.3 Hz) and δ 5.75 (J = 14.6 Hz) after brief warming of the sample. The first of these signals corresponds well with that assigned to **B** (see Table II). The other doublet has a very similar coupling constant, characteristic of ^1J(Rh–C), and is assigned to a mixed halide rhodium methyl complex, $[MeRh(CO)_2Cl_nI_{3-n}]^-$. Definitive assignment of a value of n for this species is not possible using the available data, but since it is observed very early in the reaction, it is most probably 2. The methyl ^{13}C resonance of the mixed halide species is shifted to low field relative to that of **B**, as observed for iridium analogs (Table II).

Scheme IV. Mechanism for the Reaction of $[Rh(CO)_2Cl_2]^-$ with MeI (Oxidative Addition of MeCl is Assumed To Be Negligibly Slow.)

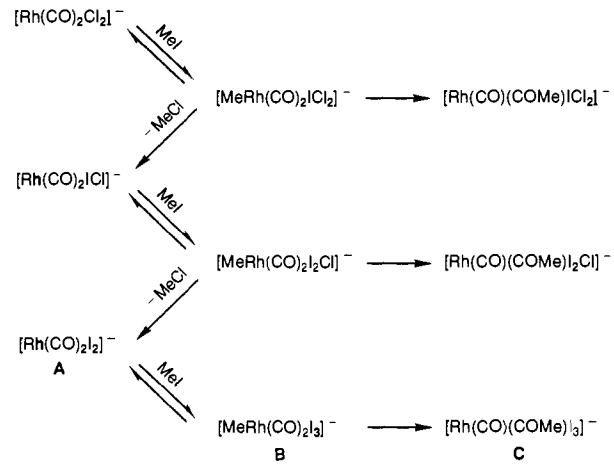

After a further period of warming, increased halide exchange was indicated by the presence of **A** as the major Rh(I) species and by the growth of the signal due to MeCl. The methyl and carbonyl signals of **B** had also grown relative to those assigned to mixed halide rhodium methyl complexes.

These ^{13}C NMR experiments show that mixed halide analogs of **B** can be generated in the reaction of $[Rh(CO)_2Cl_2]^-$ with MeI. The potential for different stoichiometries and geometries in this system leads to difficulties in definitive assignment. We have only observed signals of a maximum of three members of the series, but other signals may be hidden or too weak to observe, since this experiment approaches the sensitivity limit of the technique.

Scheme IV shows a mechanism for the overall reaction of $[Rh(CO)_2Cl_2]^-$ with MeI, where halide exchange occurs via successive oxidative addition/reductive elimination steps and migratory insertion is possible for any of the intermediate rhodium methyl complexes, giving a mixture of rhodium acyl products.

Discussion

This paper reports a detailed study of the key organometallic processes and the first quantitative measurement of the rate of the crucial C–C bond forming step in the rhodium/MeI-catalyzed carbonylation of methanol to acetic acid or of methyl acetate to acetic anhydride. The intermediate, $[MeRh(CO)_2I_3]^-$ (**B**), has now been detected, identified, and structurally characterized (as the fac,cis isomer) by a combination of FTIR and ^{13}C NMR spectroscopy, using isotopically enriched reactants. Optimum conditions for its detection involve the use of neat MeI as solvent. The high concentration of MeI increases the rate of the oxidative addition reaction forming **B**, whilst the rate of consumption of **B** via migratory insertion is slower in a medium of low polarity.

Kinetic information has been determined for each of the four rate processes illustrated in Scheme II. A complete set of rate data has been obtained at 35 °C: $k_1 = 6.8 \times 10^{-5}$ M^{-1} s^{-1} (MeI), $k_{-1} = 1.5 \times 10^{-2}$ s^{-1} (CH_2Cl_2), $k_2 = 1.33 \times 10^{-1}$ s^{-1} (MeI), and $k_{-2} = 4.20 \times 10^{-5}$ s^{-1} (MeI). Variable-temperature studies have enabled activation parameters to be determined for the overall reaction of **A** with MeI, as well as the forward (k_2) and reverse (k_{-2}) methyl migration processes (Table IV).

The reaction of MeI with the chloro analog of **A**, $[Rh(CO)_2Cl_2]^-$, has also been further examined, using the same techniques. Halide exchange between the reactants was shown to occur via a stepwise mechanism involving oxidative addition of MeI followed by reductive elimination of MeCl (Scheme IV). Direct spectroscopic evidence was obtained for intermediate mixed halide rhodium methyl complexes, $[MeRh(CO)_2Cl_nI_{3-n}]^-$, which could also undergo migratory insertion.

Reactivity of $[MeRh(CO)_2I_3]^-$ (B). Two independent sets of observations both lead to the conclusion that the high reactivity of **B** is primarily due to rapid migratory insertion, giving **C**, and that reductive elimination of MeI is relatively insignificant under the conditions of our experiments. Firstly, the kinetics of approach to steady-state behavior at the start of the reaction between **A** and MeI at 5 °C give a value of $(k_{-1} + k_2) = (8.5 \pm 0.5) \times 10^{-3}$ s^{-1}, which is very similar to k_2 alone (8.3×10^{-3} s^{-1} at 5 °C), indicating that k_2 is large compared to k_{-1}. This conclusion was confirmed by a comparison of the rate of migration of methyl between carbonyl groups in $[Rh(^{12}CO)(^{13}COMe)I_3]^-$ (**C'**) with the rate of decomposition of **C**. The first-order rate for scrambling of the isotopic label in **C'** ($k_{-2} = 4.2 \times 10^{-5}$ s^{-1}) is an order of magnitude faster than the rate of conversion of **C** into **A** and MeI ($k_b = 4.05 \times 10^{-6}$ s^{-1}). This indicates a value for the ratio k_2/k_{-1} of ca. 9 in CH_2Cl_2 at 35 °C. Thus, migratory insertion in **B** is an order of magnitude faster than reductive elimination, as previously suggested, and is the reason why **B** was not detected in earlier studies.

Equilibrium constants derived from the kinetic data at 35 °C ($K_1 = 4.5 \times 10^{-3}$ M^{-1}, $K_2 = 3.2 \times 10^3$) show that **B** is unstable with respect to both migratory insertion and reductive elimination of MeI. The high reactivity of **B** contrasts sharply with the stability of its iridium analog, $[MeIr(CO)_2I_3]^-$, which only undergoes migratory insertion at elevated temperature in the presence of carbon monoxide and is also relatively stable toward reductive elmination of MeI.[31] We have estimated that the rate of migratory insertion is 10^5 times slower for $[MeIr(CO)_2I_3]^-$ than for **B**.[32] The differences between these rhodium and iridium methyl complexes can be ascribed to the greater inertness and the stronger metal–carbon bond for a 5d transition metal complex. It has recently been suggested that a vertical step (3d → 4d or 4d → 5d) leads to an increase of 17–21 kJ mol^{-1} in the M–C bond dissociation energy.[33]

Oxidative Addition/Reductive Elimination. Activation parameters for the overall reaction of **A** with MeI (Table IV) are similar to those reported in other solvents of low polarity[12] and are consistent with rate-determining nucleophilic attack of **A** on MeI. They are also comparable with activation parameters for the overall carbonylation cycle[34] ($\Delta H^\ddagger = 63.6$ kJ mol^{-1} and $\Delta S^\ddagger = -116$ J mol^{-1} K^{-1} for methanol carbonylation;[5] $\Delta H^\ddagger = 60.2$ kJ mol^{-1} and $\Delta S^\ddagger = -113$ J mol^{-1} K^{-1} for methyl acetate carbonylation[3]).

Our data indicate that if **B** did not undergo rapid migratory insertion, the equilibrium concentration of the methyl rhodium species generated in neat MeI at 35 °C would be only ca. 7% of that of **A**. The instability of **B** with respect to loss of MeI can also be understood in terms of a relatively weak Rh–C bond in **B**. In support of this suggestion, it has been observed that the reaction of **A** with strong methylating agents such as Me_3OBF_4 leads to methylation of an iodide ligand rather than at the rhodium center.[35] It has been argued[5] on the basis of kinetic data that **A** has a Pearson nucleophilicity[36] 2 orders of magnitude lower than that of iodide ion. Thus, competition between the two nucleophiles is expected to favor formation of MeI rather than the rhodium methyl species.

Alkyl/Acyl Isomerization. The kinetic data reported in this paper represent the first quantitative measurements for migratory insertion (**B** → **C**) and deinsertion (**C** → **B**) in the rhodium-catalyzed carbonylation cycle. Comparison of k_2 and k_{-2} indicates that the equilibrium constant, K_2, for alkyl/acyl isomerization is large (10^3–10^4) under the conditions of our experiments. Thermodynamic parameters for the reaction can be obtained from the activation parameters for forward and reverse reactions (Table IV), giving $\Delta H = -37$ kJ mol^{-1} and $\Delta S = -54$ J mol^{-1} K^{-1}. Extrapolation to the operating temperature for carbonylation (180 °C) leads to a much lower value of $K_2 \approx 30$, indicating that **C** becomes less favored with respect to **B** at elevated temperatures. However, under catalytic conditions, trapping of **C** by CO is likely to be efficient (see Scheme I).

The position of alkyl/acyl equilibria in rhodium complexes has been shown to vary depending on the solvent, ligand environment, charge, and nature of the migrating alkyl group.[37-39] However, it is common for the equilibrium to be attained rapidly, indicating that methyl migration on rhodium centers is a facile process. The rate of migratory insertion observed in this system is at least an order of magnitude faster than previously reported for other unactivated metals in solvents of low polarity.[16] The relative ease of migratory insertion on a rhodium center, compared, for example, with iridium, clearly contributes significantly to the ability of rhodium to promote carbonylation processes. The present results also suggest that the high selectivity,[5] with respect to unwanted side reactions such as methane formation, is favored not only by rapid migratory insertion in **B** but also because the potential equilibrium concentration of the methyl species is much lower for rhodium than for iridium.

Acknowledgment. We thank David Gulliver and Glenn Sunley for helpful discussion and Miss Jean Pearson for providing spectroscopic data for model iridium complexes. We also thank BP Chemicals, the SERC, and the University of Sheffield for generous support of this work and Johnson Matthey for the loan of some rhodium chloride.

(31) Forster, D. *J. Chem. Soc., Dalton Trans.* **1979**, 1639.
(32) Bassetti, M.; Monti, D.; Haynes, A.; Pearson, J. M.; Stanbridge, I. A.; Maitlis, P. M. *Gazz. Chim. Ital.* **1992**, *122*, 391.
(33) Mancuso, C.; Halpern, J. *J. Organomet. Chem.* **1992**, *428*, C8.
(34) In comparing activation parameters for our model system with those for overall carbonylation, the large difference in reaction medium should be noted.
(35) The products of this reaction are MeI and $[Rh(CO)_2I]_2$ in weakly coordinating solvents. In acetonitrile, the second iodide ligand can be methylated, giving $[Rh(CO)_2(NCMe)_2]^+$.
(36) Pearson, R. G.; Sobel, H.; Songstad, J. *J. Am. Chem. Soc.* **1968**, *90*, 319.
(37) Douek, Z.; Wilkinson, G. *J. Chem. Soc. A* **1969**, 2604. Franks, S.; Hartley, F. R.; Chipperfield, J. R. *Inorg. Chem.* **1981**, *20*, 3238.
(38) Bennett, M. A.; Jeffery, J. C.; Robertson, G. B. *Inorg. Chem.* **1981**, *20*, 323. Egglestone, D. L.; Baird, M. C.; Lock, C. J. L.; Turner, G. *J. Chem. Soc., Dalton Trans.* **1977**, 1576.
(39) Bassetti, M.; Sunley, G. J.; Fanizzi, F. P.; Maitlis, P. M. *J. Chem. Soc., Dalton Trans.* **1990**, 1799. Kang, J. W.; Maitlis, P. M. *J. Organomet. Chem.* **1971**, *26*, 393. Hart-Davis, A. J.; Graham, W. A. G. *Inorg. Chem.* **1970**, *9*, 2658.